Spectroscopy and Photophysics of Bifunctional Proton Donor–Acceptor Indole Derivatives

7 AUTHORS, INCLUDING:

Volha Vetokhina
Polish Academy of Sciences
10 PUBLICATIONS **39** CITATIONS

Teodozja Lipinska
Siedlce University of Natural Sciences and Hu…
16 PUBLICATIONS **46** CITATIONS

J. Waluk
Polish Academy of Sciences
257 PUBLICATIONS **3,690** CITATIONS

Jerzy Herbich
Instytut Chemii Fizycznej PAN
46 PUBLICATIONS **1,100** CITATIONS

Spectroscopy and Photophysics of Bifunctional Proton Donor–Acceptor Indole Derivatives

Volha Vetokhina,[†] Michał Kijak,[†] Teodozja M. Lipinska,[‡] Randolph P. Thummel,[§] Jerzy Sepiol,[†] Jacek Waluk,[†,⊥] and Jerzy Herbich*[,†,⊥]

[†]Institute of Physical Chemistry, Polish Academy of Sciences, Kasprzaka 44/52, 01-224 Warsaw, Poland
[‡]Institute of Chemistry, Siedlce University of Natural Sciences and Humanities, 3 Maja 54, 08-110 Siedlce, Poland
[§]Department of Chemistry, University of Houston, Houston, Texas 77204-5003, United States
[⊥]Faculty of Mathematics and Science, Cardinal Stefan Wyszyński University, Dewajtis 5, 01-815 Warsaw, Poland

ABSTRACT: We report spectroscopic and photophysical studies of a series of selected indole derivatives in solutions and under supersonic jet isolation conditions. All the compounds can assume two rotameric forms, *syn* and *anti*. The bifunctional molecules containing both the hydrogen bond donor (indole NH group) and acceptor centers (oxygen, nitrogen, or sulfur atoms) located in separate moieties covalently linked by a single bond are compared with the compound that does not have any acceptor center, 2-(1*H*-pyrrol-2′-yl)-1*H*-indole. The former compounds (containing furan, thiazole, or thiophene moieties) were anticipated to show solvent-dependent photophysics. Contrary to the expectations, all the compounds reveal very efficient fluorescence, independent of solvent polarity and hydrogen bond donor and acceptor abilities. Laser spectroscopic studies combined with supersonic jet techniques and quantum chemical computations have been performed in order to identify the rotameric forms and to gain insight into the changes in the molecular structure accompanying electronic excitation.
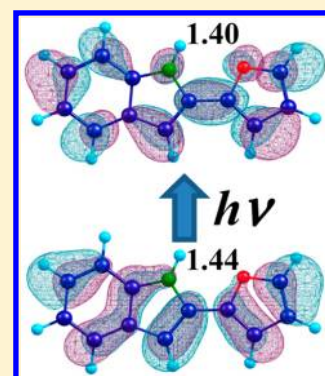
1. INTRODUCTION

A special class of bifunctional molecules consists of compounds for which the hydrogen bond donor and acceptor centers are located in separate moieties, connected by a single bond (for example, 2-(2′-pyridyl)indole (**2-PI**) and 2-(2′-pyridyl)pyrrole (**PP**)). Such structure often lead to an appearance of two rotameric forms, *syn* and *anti*, with both centers on the same or on the opposite sides of the molecule, respectively. The two conformers, of which the relative fractions are often solvent dependent, may reveal drastically different excited state properties.[1−5] Detailed understanding of the mechanisms responsible for *syn−anti* equilibria may, therefore, lead to applications of bifunctional molecules, e.g., as probes of solvent polarity and/or proticity.

A general scheme showing the solvent-induced rotamerization and excited-state deactivation channels in bifunctional heteroazaromatic molecules such as **2-PI**[2,5] and **PP**[5] has been proposed previously. In nonpolar solvents only the *syn* species should be present (this rotamer predominantly exists in the gas phase in supersonic jets[6,7]). This form can undergo excited-state intramolecular proton transfer (ESIPT) process depending on the mutual arrangement of the proton donor and acceptor centers. A small fraction of the *anti* form can be expected in polar aprotic solvents, while in alcohols it becomes significant. The stabilization of the *anti* structure is due to a larger ground state dipole moment and stronger and more linear hydrogen bonds with hydroxylic partners than in the *syn* species.[2,5] In some cases (as for 2-(2′-pyridyl)indoles) the *anti* conformer can be more stable in alcohol solutions than the *syn*

one because of a stabilization of the *anti* structure by two separate alcohol molecules connected to the opposite sides of a chromophore. In alcohols and water the excited state of the *syn* conformer is rapidly depopulated due to a formation of cyclic hydrogen-bonded complexes with a protic partner. The deactivation may involve $S_1 \rightarrow S_0$ enhanced internal conversion and/or fast excited-state double proton transfer (ESDPT). The latter process occurs in 1:1 complexes on a time scale of single picoseconds or faster, whereas the former involves complexes with two (or more) molecules of alcohol (1:*n* complex), and takes much longer (tens to hundreds of picoseconds).[8] The lack of tautomeric fluorescence in alcohols combined with quenching of the primary fluorescence indicates a domination of complexes other than those of cyclic structure and 1:1 stoichiometry.

In this work we describe studies of selected bifunctional indole derivatives for which the hydrogen bond donor (the indole NH group) and the acceptor centers are located in separate moieties, covalently linked by a single bond (Scheme 1). The aim of this work is to compare spectroscopy and photophysics of the compounds which can form *syn* (with the donor and the acceptor on the same side) and *anti* (with the two groups on the opposite sides) conformers via internal rotation around a single bond (2-(thiophen-2′-yl)-1*H*-indole (**THOIN**), 2-(thiazol-2′-yl)-1*H*-indole (**THAIN**), and 2-

Scheme 1. Structures and Acronyms of the Studied Indole Derivatives[a]
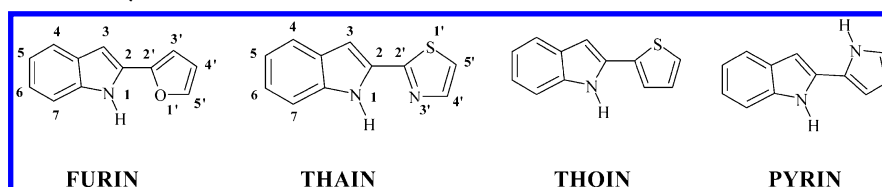
[a]The compounds are shown in the most stable ground state conformation.

(furan-2′-yl)-1H-indole, **FURIN**), with the compound that does not have any acceptor center, 2-(1H-pyrrol-2′-yl)-1H-indole (**PYRIN**). Due to the fact that only the *syn* rotamers of bifunctional molecules are able to form cyclic, doubly hydrogen bonded dimers or complexes with protic partners, it was expected that the former three molecules, but not the latter compound, should exhibit solvent-dependent photophysics. This group of compounds was especially synthesized to study the effects of electronegativity of the hydrogen bond acceptor centers (oxygen, nitrogen, or sulfur atoms) on their photophysical properties.

2. EXPERIMENTAL SECTION

We attempted to prepare 2-(thiophen-2′-yl)-1H-indole and 2-(furan-2′-yl)-1H-indole using the Fischer indole synthesis under conditions elaborated earlier by us for 2-(pyrid-2′-yl)indoles.[9,10] Starting materials, 2-acetylthiophene or 2-acetylfurane, were converted to appropriate phenylhydrazones, and, in the next step, to the indole moiety. The syntheses were carried out in 0.16 M zinc chloride solution in triethylene glycol (TEG) under controlled microwave heating. However, this method was unsuccessful for the preparation of 2-(1H-pyrrol-2′-yl)-1H-indole, which we obtained by the excellent method of Bocchi and Palla[11] from 3-bromoindole and pyrrole. The details of the syntheses will be published elsewhere.

The 2-(thiazol-2′-yl)-1H-indole was prepared as follows: A mixture of 2-acetylthiazole (1.27 g, 10.0 mmol), phenylhydrazine (1.30 g, 12.0 mmol), and glacial HOAc (4 drops) in absolute EtOH (10 mL) was refluxed for 5 h. Evaporation of the solvent and chromatography on alumina, eluting with CH_2Cl_2/petroleum ether (1:1), provided a mixture of *E* and *Z* isomers (2.16 g, 99%). This hydrazone mixture (1.67 g, 7.7 mmol), $ZnCl_2$ (5.44 g), and glacial HOAc (110 mL) were refluxed under Ar. After 24 h, additional $ZnCl_2$ (2.72 g) was added, and reflux was continued for 48 h. After being cooled, the reaction mixture was concentrated and the residue was dissolved in CH_2Cl_2 (50 mL) and 10% NaOH was added until pH 14 was obtained. The mixture was sonicated for 15 min and the white residue filtered. The two layers were separated and the aqueous phase was extracted with CH_2Cl_2 (3 × 50 mL). The combined organic phase was washed with brine (50 mL), dried ($MgSO_4$), and concentrated. Chromatography on silica gel, eluting with CH_2Cl_2, provided 2-(2′-thiazolyl)indole (0.92 g, 56%) as a white solid: mp 125−126 °C; ^1H NMR (CDCl$_3$) δ 9.65 (br s, 1H), 7.81 (d, 1H, *J* = 3.3 Hz), 7.65 (d, 1H, *J* = 7.8 Hz), 7.40 (dd, 1H, *J* = 8.1, 1.2 Hz), 7.32 (d, 1H, *J* = 3.3 Hz), 7.26 (td, 1H, *J* = 8.1, 1.2 Hz), 7.13 (td, 1H, *J* = 7.8, 1.5 Hz), 7.04 (dd, 1H, *J* = 1.8, 0.9 Hz); ^{13}C NMR (CDCl$_3$) δ 161.6, 142.7, 137.2, 131.5, 128.5, 124.0, 121.4, 120.5, 118.5, 111.7, 103.6 ppm.

The solvents used for our studies—*n*-hexane (HEX), ethyl acetate (EA), acetonitrile (ACN), 1-propanol, and 1-butanol—were of spectroscopic or fluorescence grade (Aldrich or

Merck). All solvents were checked for the presence of fluorescing impurities.

Electronic absorption spectra were recorded on a Shimadzu UV 3100 spectrophotometer. Stationary fluorescence and fluorescence excitation spectra were obtained with an Edinburgh FS 900 CDT spectrofluorometer. The spectra were corrected by using the spectral sensitivity curves of the instrument. Fluorescence spectra were recorded as a function of wavelength (λ) and subsequently multiplied by a factor of λ^2 in order to convert counts per wavelength into counts per wavenumber. For the quantum yield determinations, the solutions had identical optical densities at the excitation wavelength. For the determination of quantum yields, quinine sulfate in 0.05 mol dm^{-3} H_2SO_4 was used as a standard (φ = 0.51).[12]

Fluorescence decay lifetimes were measured by using time-resolved single photon counting on an Edinburgh FL 900 CDT spectrofluorometer with an estimated time resolution of about 500 ps.

A homemade spectrometer used for obtaining LIF and dispersed fluorescence (DF) spectra has been described previously.[13,14] In our case the samples were heated to 370 K. They were diluted by 3 atm of helium and injected via a modified high temperature pulsed nozzle (General Valve 9) through an orifice (0.5 or 0.2 mm in diameter). LIF and SVLF experiments were carried out with use of an optical parametric oscillator (OPO, Continuum, Sunlite LX) pumped by the third harmonic of a Nd/YAG laser (Continuum, Powerlite 8010). The tunable excitation pulses in the UV range were produced by doubling red radiation generated from the OPO in KDP crystal. Fluorescence from the sample was collected by a toroidal mirror and directed by a flip-flop plane mirror to a Hamamatsu R2949 photomultiplier connected to a Yokogawa DL9140 oscilloscope to measure LIF spectra or to a slit of a Sciencetech, model 9040 spectrograph with an Andor iDUS CCD camera to accumulate DF spectra.

All calculations were performed with use of the Gaussian 09[15] suite of programs. Ground state geometries were optimized by using density functional theory (DFT) with B3LYP (Becke, Lee, Yang, and Parr three-parameter) hybrid functional.[16,17] The electronic transition energies were obtained by time-dependent DFT (TD-DFT) formalism. For the excited state geometry optimizations TD-DFT and configuration interaction singles (CIS) procedures were used. In all cases the double-ζ 6-31+G(d,p) basis set was applied. For all the stationary points frequencies have been calculated to check if the geometry corresponds to the energy minimum. The Franck−Condon analysis, with Herzberg−Teller approximation (FCHT) for absorption, implemented in the Gaussian 09 package was used to compute vibrationally resolved absorption and emission spectra. The frequency scaling factors of 0.964 (DFT/TD-DFT) and 0.92 (CIS) were applied throughout the paper.

3. RESULTS AND DISCUSSION

To estimate the relative ground state energies of the rotameric forms, theoretical calculations at the B3LYP/6-31+G(d,p) level were performed (Table 1). The predicted low energy ground

Table 1. Ground and Excited State Data: Relative Energies (computed at the DFT/B3LYP/3-61+G(d,p) level) of the Various Rotameric and Tautomeric Forms (ΔE), Dipole Moments (μ_g and μ_e, respectively), and Dihedral Angles between Proton Donating and Accepting Moieties

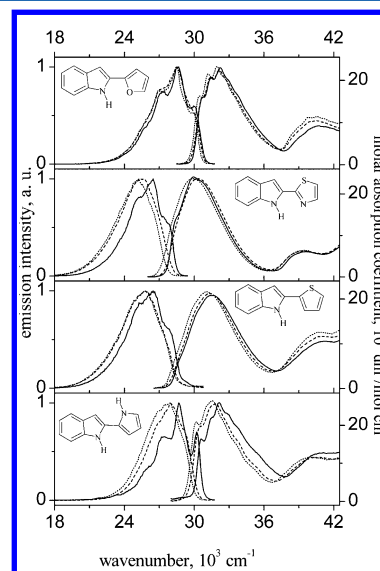|			FURIN	THAIN	THOIN	PYRIN
S_0	ΔE, kcal/mol	syn	0.0	0.0	0.1	1.6
		anti	1.1	3.1	0.0	0.0
		taut		23.9		
	μ_g, D	syn	2.0	1.4	1.8	2.6
		anti	2.5	2.5	2.2	1.7
		taut		6.6		
	dihedral angle	syn	0.0°	0.0°	27.9°	33.3°
		anti	0.0°	0.0°	23.2°	22.4°
		taut		0.0°		
			TD-DFT	TD-DFT	TD-DFT	TD-DFT
S_1	ΔE, kcal/mol	syn	0.0	0.0	0.3	1.3
		anti	2.0	4.0	0.0	0.0
		taut		−7.9		
	μ_e, D	syn	0.8	3.4	2.0	3.1
		anti	1.9	3.6	3.0	1.8
		taut		1.8		
	dihedral angle	syn	0.0°	0.0°	0.0°	7.3°
		anti	0.0°	0.0°	0.0°	4.0°
		taut		1.6°		

state species of **THAIN** and **FURIN** under vacuum isolation conditions correspond to the planar *syn* forms due to their stabilization by intramolecular hydrogen bond. For **PYRIN** and **THOIN** the predicted lowest energy species are *anti* rotameric forms, with the dihedral angles of 22.4° and 23.2°, correspondingly. Their *syn* conformers are also nonplanar. The nonplanar structure of **PYRIN** can be explained by strong repulsive interactions of the NH hydrogen atoms that do not allow the compound to become planar. The computed energy gaps between *syn* and *anti* conformers, however, are small; the values change from 0.1 kcal/mol for **THOIN** to −3.1 kcal/mol for **THAIN**.

Additional calculations were performed for the tautomeric form of **THAIN** which show relatively large destabilization energy of 23.9 kcal/mol of this form with respect to the *syn* rotamer (noteworthy, **FURIN** and **THOIN** are not able to form the tautomeric species, in which the proton is shifted from the indole nitrogen atom onto the furan oxygen atom or onto the thiophene sulfur atom, respectively). The computed ground state dipole moment values μ_g of the *syn* and *anti* forms are in the range from 1.4 to 2.6 D.

Computations at the TD-DFT/6-31+G(d,p) level predict a similar situation for the lowest energy species, *syn* for **FURIN** and **THAIN**, and *anti* for **THOIN** and **PYRIN**. The stabilization energy spans the range from 0.3 kcal/mol (**THOIN**) to −4.0 kcal/mol (**THAIN**). Both compounds (**THOIN** and **PYRIN**), nonplanar in the ground state, have a tendency to flatten upon excitation (**THOIN** becomes totally planar). Similarly to **2-PI** and **PP**, the tautomeric form of **THAIN** is predicted to be significantly stabilized in the excited state. The ab initio computations at the CIS/6-31+G(d,p) level

predict that in the excited state the *syn* rotamer is relatively stabilized for all the compounds under study. The stabilization energy, however, which is significant (ca. 3.1 kcal/mol) for **FURIN** and **THAIN**, seems to be negligibly small for **PYRIN** and **THOIN**. As was the case of DFT computations, **THOIN** and **PYRIN** have a tendency to flatten upon excitation.

The absorption and fluorescence spectra of the indole derivatives recorded in three solvents (*n*-hexane, acetonitrile, and 1-propanol, i.e. representing nonpolar, polar aprotic, and protic media, respectively) are presented in Figure 1. The corresponding spectroscopic and photophysical data are collected in Tables 2 and 3.

Figure 1. Room temperature absorption and corrected and normalized fluorescence spectra of **FURIN**, **THAIN**, **THOIN**, and **PYRIN** (from top to bottom). Full lines, *n*-hexane; dashed lines, acetonitrile; dotted lines, 1-propanol.

The shape and spectral positions of the broad absorption and emission spectra of **PYRIN** and **FURIN** are very similar: two lowest absorption bands and the single emission spectra in various solvents are located at about 32 000, 41 000, and 28 500 cm^{-1}, respectively. The spectra of sulfur-containing compounds, **THAIN** and **THOIN**, are considerably red-shifted. The Stokes shift values vary from ca. 3700(±100) cm^{-1} for **FURIN** and **PYRIN** to about 5400(±300) cm^{-1} for **THOIN**.

The fluorescence excitation spectra of **FURIN**, **THAIN**, **THOIN**, and **PYRIN** in *n*-hexane and 1-propanol, as well as in acetonitrile, match well the corresponding absorption spectra. This finding indicates that the fluorescence originates from the same species which exist in the ground state. The absorption and emission spectra of all the compounds under study, in agreement with the small values of the computed ground and excited state dipole moments (0.8−3.6 D), do not show any significant solvent dependence.

Contrary to our expectations, the photophysical data of **FURIN**, **PYRIN**, **THAIN**, and **THOIN** do not show any solvent dependence (Table 2). The fluorescence quantum yields Φ_f are high (ca. 20% for the latter two compounds and ca. 80% for **FURIN** and **PYRIN**). The four times smaller Φ_f values for the sulfur containing compounds most probably manifest the increase of the efficiency of the intersystem crossing processes (leading to the increase of population of the

Table 2. Solvent Effects on the Spectral Positions of the Absorption and Fluorescence Maxima ($\tilde{\nu}_{abs}$ and $\tilde{\nu}_{fl}$, correspondingly, cm^{-1}), Quantum Yields (Φ_f), Decay Times (τ ns), and the Resulting Radiationless (k_{nr}, s^{-1}) and Radiative (k_f, s^{-1}) Rate Constants, and Electronic Transition Dipole Moments in Absorption (M_{abs}, D), and Fluorescence (M_{fl}, D)

compd	solvent	$\tilde{\nu}_{abs}$[b]	$\tilde{\nu}_{fl}$[b]	Φ_f[a]	τ[a]	$k_r \times 10^8$	$k_{nr} \times 10^8$	M_{fl}	M_{abs}
FURIN	HEX	32 300	28 600	0.78	1.4	5.6	1.6	5.4	4.3
	ACN	32 250	28 600	0.87	1.6	5.4	0.8	5.5	4.4
	1-PrOH	32 000	28 500	0.89	1.7	5.2	0.6	5.2	4.7
THAIN	HEX	29 900	26 400	0.23	~0.6	~3.8	~12.8	~5.0	4.9
	ACN	30 300	25400	0.24	0.9	2.7	8.4	4.6	5.0
	1-PrOH	29 800	25 200	0.18	~0.6	~3.0	~13.7	~4.7	5.0
THOIN	HEX	31 550	26 400	0.22	~0.8	~2.8	~9.8	~4.3	4.7
	ACN	31 400	25 700	0.25	0.9	2.8	8.3	4.6	4.8
	1-PrOH	31 100	25 700	0.27	1.0	2.7	7.3	4.4	4.7
PYRIN	HEX	32 200	28 700	0.72	1.2	6.0	2.3	5.6	4.4
	ACN	31 800	28 000	0.84	1.6	5.3	1.0	5.6	4.5
	1-PrOH	31 500	27 800	0.89	1.6	5.6	0.7	5.6	4.2

[a]Estimated error: 10%. Thus, the maximum error is about 20% for the rate constants k_{nr} and k_f and about 10% for the transition moment M_{fl}.
[b]Scatter of results: ±150 cm^{-1}.

Table 3. Comparison between TD-DFT/B3LYP/6-31+G(d,p) Calculated Energies ($\tilde{\nu}$, cm^{-1}) and Oscillator Strengths (f) Corresponding to the Vertical Transitions to Low-Lying $^1(\pi,\pi^*)$ States[a] of the Syn and Anti Forms of the Studied Compounds, and Locations of the Experimental Absorption Band Maxima ($\tilde{\nu}_{exp}$, cm^{-1}) and Molar Absorption Coefficients (ε, dm^3 mol^{-1}cm^{-1}) in n-Hexane

compd	state	$\tilde{\nu}$ syn	f syn	state	$\tilde{\nu}$ anti	f anti	$\tilde{\nu}_{exp}$[b]	ε
FURIN	S_1	31 650	0.676	S_1	31 940	0.688	32 300	23 000
	S_2	34 270	0.093	S_2	34 390	0.087		
	S_4	38 970	0.052	S_3	39 150	0.059	41 000	9 200
	S_6	42 060	0.129	S_6	41 590	0.119		
THAIN	S_1	29 130	0.392	S_1	29 420	0.504	29 900	24 100
	S_2	31 150	0.285	S_2	31 400	0.208		
	S_6	40 780	0.064	S_7	36 650	0.035	39 500	6 400
THOIN	S_1	30 500	0.512	S_1	30 280	0.507	31 550	20 800
	S_2	33 360	0.115	S_2	33 200	0.126		
	S_6	41 030	0.056	S_6	40 700	0.091	41 000	10 500
PYRIN	S_1	33 170	0.591	S_1	32 800	0.665	32 200	26 000
	S_4	39 400	0.101	S_5	39 440	0.137	40 500	12 700
	S_5	39 860	0.088	S_8	41 200	0.061		

[a]Only transitions of significant intensity are shown ($f > 0.03$). [b]Scatter of results: ±150 cm^{-1}.

triplet manifold) due to a "heavy atom effect".[18] Fluorescence decay times obtained on the nanosecond time scale can be well fitted to a monoexponential decay; the lifetime values τ are of about 0.5−1.0 ns for **THAIN** and **THOIN**, and about 1.2−1.7 ns for **FURIN** and **PYRIN**.

The obtained quantum yields (Φ_f) and lifetimes (τ) lead to large values of the radiative k_f rate constants (eq 1) as well as those of the electronic transition dipole moments in fluorescence M_{fl} (obtained in the electric dipole approximation, eq 3)[19,20]

$$k_f = \Phi_f/\tau \tag{1}$$

$$k_{nr} = (1 - \Phi_f)/\tau \tag{2}$$

$$k_f = \frac{64\pi^4}{3h}(n\tilde{\nu}_{fl})^3|\vec{M}_{fl}|^2 \tag{3}$$

where k_{nr} is the radiationless rate constant, h is the Planck constant, n is the refractive index of a solvent, and $\tilde{\nu}_{fl}$ is the wavenumber of fluorescence maximum.

This finding indicates that the radiative transitions in emission are fully allowed. Moreover, the M_{fl} values are similar

to those of the electronic transition dipole moments M_{abs} related to the lowest $^1(\pi,\pi^*) \leftarrow S_0$ absorption band (eq 4)[20]

$$|\vec{M}_{abs}|^2 = \frac{3\ln 10hc}{8\pi^3 N_A n\tilde{\nu}_{abs}} \int \varepsilon(\tilde{\nu}) \, d\tilde{\nu} \tag{4}$$

where $\varepsilon(\tilde{\nu})$ is the molar absorption coefficient at wavenumber $\tilde{\nu}$, $\tilde{\nu}_{abs}$ is the wavenumber of absorption maximum, N_A is the Avogadro number, and c is the speed of light. This observation indicates a similar nature of the Franck−Condon excited states initially reached in absorption and the solvent-equilibrated fluorescent states.

It should be stressed that **FURIN**, **THAIN**, and **THOIN**, contrary to the other bifunctional molecules for which the proton donor and acceptor groups are located in separate moieties linked by a single bond (such as 2-(2′-pyridyl)-indole,[1,2] 2-(2′-pyridyl)pyrroles,[4,7,21,22] and 2-pyridylpyra-zoles[23,24]), do not reveal any spectral and kinetic evidence of rotamerization (for all the compounds) and/or photoinduced tautomerization processes. The lack of the efficient deactivation of the lowest excited singlet states S_1 in protic media via internal conversion (IC) and/or ESDPT processes suggests that the studied compounds do not form cyclic, doubly
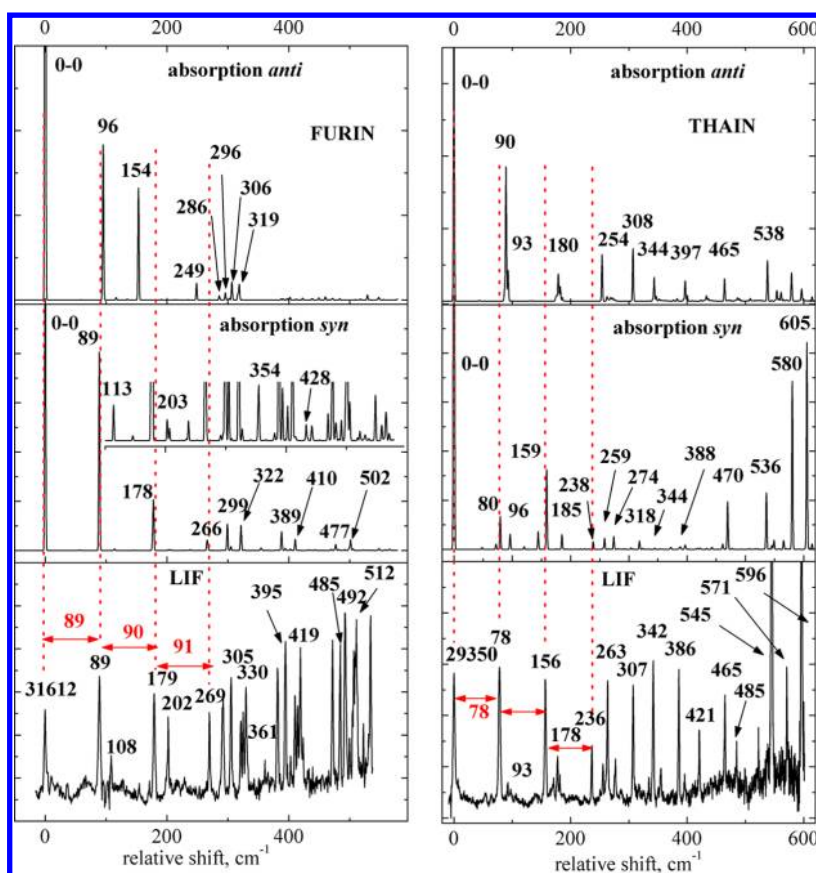
Figure 2. LIF excitation (bottom) and the absorption spectra (middle, *syn*; top, *anti*) of **FURIN** (left) and **THAIN** (right) calculated at the DFT/TD-DFT/B3LYP/6-31+G(d,p) level. Scaling factor: 0.964.[25,26] The inset presents the enlarged spectrum (intensity ×100).

hydrogen-bonded complexes. To gain more insight into the formation of the complexes, titration experiments have been performed. Upon adding 1-butanol, at concentrations low enough to prevent the formation of alcohol oligomers,[1] to an *n*-hexane solution of **THAIN** and **PYRIN** an isosbestic point in the absorption spectra is observed. This fact demonstrates an equilibrium between two individua in the ground state, most probably between the uncomplexed and complexed forms.[1] The absorption data yield the 1:1 stoichiometry of the complex of **PYRIN** and the equilibrium constant of 30(±5) dm^3 mol^{-1}. On the other hand, the analysis of the absorption of **THAIN** complexes does not lead to the unequivocal results. The analysis performed in the low-energy range of the absorption spectra (at ~27 300 cm^{-1}) results in the 1:1 stoichiometry, the determination of stoichiometry from the absorption data at ~30 500 cm^{-1} and ~28 570 cm^{-1} lead to the values of 1:1.4 and 1:1.6, respectively. The latter findings can hardly be explained in terms of the model assuming a reaction involving one chromophore molecule and *n* alcohol molecules,[1] but this result is most likely related to the errors caused by small absorption changes upon adding alcohol. For **THOIN** and **FURIN** no measurable changes in absorption were observed in a wide range of alcohol concentrations. The fluorescence spectra of **THAIN**, **THOIN**, and **PYRIN** show a small shift to lower energies with the increase of 1-BuOH concentration; the emission intensities, however, do not change significantly.

The TD-DFT computed spectral positions of transitions to the lowest excited $^1(\pi,\pi^*)$ states of the *syn* and *anti* rotameric forms of all the compounds under vacuum isolation conditions are in excellent agreement with the experimentally measured

absorption maxima (Table 3). It should be stressed, however, that the computed energies and oscillator strengths of the low-lying vertical transitions of both rotameric forms of each compound are very similar. Therefore, the position and intensities of the near-UV experimental absorption bands do not allow us to distinguish which forms of the compounds exist in the ground state. The lowest computed transitions S$_1$ ← S$_0$ for all the compounds are dominated by a configuration corresponding to an electron jump from the highest occupied molecular orbital (HOMO) to the lowest unoccupied molecular orbital (LUMO). These L$_a$ ← S$_0$ type transitions carry high oscillator strength.

In an attempt to identify rotameric forms and to gain more insight into the changes accompanying electronic excitation of **FURIN** and **THAIN** (as representatives of the studied indole derivatives) high resolution spectroscopic investigations under supersonic jet isolation conditions have been performed. The experimental laser-induced fluorescence (LIF) excitation (which provides information about vibrational frequencies in the lowest excited singlet state S$_1$) and dispersed fluorescence (DF) spectra (showing vibrational frequencies in the ground state S$_0$), obtained for excitation into specific vibronic level (SVLF) of bare molecules, are compared with the DFT/TD-DFT calculated absorption and emission spectra obtained by the Franck−Condon analysis. The 0−0 regions of the LIF and DF spectra of **FURIN** and **THAIN** show a rich pattern of low-frequency vibrations (Figure 2). The origins of the S$_1$ ← S$_0$ transitions are assigned to the lowest energy bands of the LIF spectra which are observed at 31 612(±1) and 29 350(±1) cm^{-1}, respectively. The 0−0 bands of the LIF spectra of both

Table 4. Transition Energies (cm^{-1}) and Tentative Assignments ($\Delta\tilde{\nu}_{calc}$ computed at the TD-DFT (in parentheses) and CIS/B3LYP/6-31+G(d,p) levels) of the Vibronic Transitions ($\Delta\tilde{\nu}_{exp}$) in the Low-Energy Part of the LIF Excitation Spectra^b of FURIN and THAIN

	FURIN				THAIN		
		$\Delta\tilde{\nu}_{calc}{}^c$				$\Delta\tilde{\nu}_{calc}{}^c$	
$\Delta\tilde{\nu}_{exp}$	assign.^{a}	syn	anti	$\Delta\tilde{\nu}_{exp}$	assign.^{a}	syn	anti
31 612	0−0	31 645	31 940	29 350	0−0	29 130	29 415
89	**A**	**94 (89)**	**98 (96)**	78	**A**	**88 (80)**	**93 (90)**
108	2 × B	50 (57) × 2	56 (58) × 2	93	2 × B	50 (48) × 2	46 (49) × 2
179	2 × **A**			156	2 × **A**		
202	**A** + 2 × B or 2 × C	98 (89) × 2	83 (77) × 2	171	**A** + 2 × B?		
216	4 × B			178	**A** + 2 × B or 2 × C	87 (72) × 2	68 (43) × 2
269	3 × **A**			236	3 × **A**		
293	2 × **A** + 2 × B or **A**+2 × C			255	2 × **A** + 2 × B or **A** + 2 × C		
305	**D**	**312 (299)**	**315 (306)**	263	**D**	**270 (259)**	**270 (254)**
321	**A** + 4 × B?			277	−		
325	6 × B			307	**E**	**318 (308)**	**319 (308)**
330	**E**	**333 (322)**	**337 (319)**	335	3 × **A** + 2 × B or 2 × **A** + 2 × C		
361	4 × **A**			342	**A** + **D**		
381	3 × **A** + 2 × B or 2 × **A** + 2 × C			355	2 × B + **D**		
395	**A** + **D**			386	**A** + **E**		
413	2 × B + **D**			396	2 × B + **E**		
419	**A** + **E**			421	2 × **A** + **D**		
439	2 × B + **E**			465	2 × **A** + **E**		
472	4 × **A** + 2 × B or 3 × **A** + 2 × C			485	**F**	**488 (470)**	**489 (465)**
485	2 × **A** + **D**			522	−		
492	−			545	**G**	**560 (536)**	**558 (538)**
~508	2 × **A** + **E**			571	**H**	**595 (580)**	**592 (580)**
512	**F**	**522 (502)**	**523 (505)**	596	**I**	**623 (605)**	**622 (596)**

^{a}Bold, in-plane vibrations; normal, out-of-plane vibrations. ^{b}Estimated error: 17 cm^{-1}.[7] ^{c}Scaling coefficients: 0.964 (DFT) and 0.92 (CIS).[25,26]
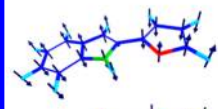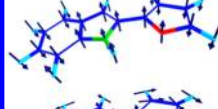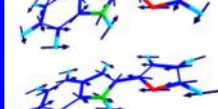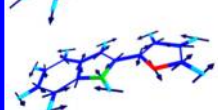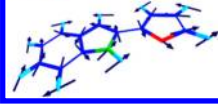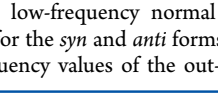

Figure 3. Forms of several low-frequency normal modes of **FURIN** with DFT/B3LYP/6-31+G(d,p) (S$_0$) or TD-DFT and CIS/B3LYP/6-31+G(d,p) (S$_1$) computed (for the *syn* and *anti* forms) and experimental (in bold) frequency values (cm^{-1}) for the ground (S$_0$) and fluorescent (S$_1$) state. The experimental frequency values of the out-of-plane vibrations correspond to the first even overtones.

compounds are found to be relatively strong, which suggests that no dramatic structural changes in **FURIN** and **THAIN** take place upon 0−0 excitation to the S$_1$ state. TD-DFT calculations predict the positions of the S$_1$ ← S$_0$ vertical transitions of **FURIN** at 31 645 cm^{-1} for the *syn* rotameric form

and at 31 940 cm^{-1} for the *anti* one; the computed values are very similar and both are in a very good agreement with the experimental value. The same situation is observed for **THAIN**: the computed values of the S$_1$ ← S$_0$ vertical transitions at 29 130 cm^{-1} for the *syn* and at 29 415 cm^{-1} for the *anti* rotameric

forms do not allow us to distinguish between both rotameric forms.

The comparison of the experimental LIF spectra with the DFT/TD-DFT computed absorption spectra suggest that the LIF spectra of **FURIN** and **THAIN** monomer correspond to the *syn* forms. For example, the spectral positions of the **FURIN** bands observed at 89, 179, and 270 cm^{-1} are in a very good agreement with the bands at 89, 178, and 266 cm^{-1} theoretically predicted for the *syn* form. For **THAIN**, theoretically predicted spectral positions of the vibronic bands at 80, 159, and 238 cm^{-1} for the *syn* rotamer correspond to the ones experimentally observed at 78, 156, and 236 cm^{-1}, respectively. The computed absorption spectra of the *anti* forms of both compounds do not show these bands.

The spectral positions of the other bands observed in the computed absorption of the *syn* form fit satisfactorily to the LIF spectra. On the basis of theoretical computations tentative vibrational assignments are proposed in Table 4. The calculations predict that the compounds should be planar in both S$_0$ and S$_1$ states. **FURIN** exhibits 63 fundamental transitions, 43 of those are due to in-plane polarized (a′) ones, whereas 20 correspond to out-of-plane (a′) vibrations. **THAIN** has 60 normal modes, 41 of a′ and 19 of a′ symmetry. Due to the fact that the lowest excited singlet states of the compounds are of $^1(\pi,\pi^*)$ character (the $^1(n,\pi^*)$ states are predicted to lie higher than 40 000 cm^{-1}) only totally symmetric, in-plane a′ vibrations are expected to appear in the LIF and SVLF spectra. The transitions involving odd quanta of out-of-plane vibrations are nontotally symmetric and thus symmetry forbidden. Thus, only even overtones of the latter vibrations are expected to be observed in the experimental spectra.

The transitions of **FURIN** (Table 4) observed at 89 (A), 305 (D), 330 (E), and 512 cm^{-1} (F) from the origin most probably correspond to the in-plane modes which are visualized in Figure 3. The spectrum shows also their overtones at 179, 269, and 361 cm^{-1}. A most prominent is the progression built on the 0−0 transition by the in-plane C2−C2′ rocking vibration. Combinations (the bands at 395 cm^{-1}, 485 cm^{-1}, as well as 419 cm^{-1} and ~508 cm^{-1}) are assigned to the progressions of the 89 cm^{-1} vibration built on the 305 and 330 cm^{-1} fundamental transitions, respectively. Under assumption that even overtones of out-of-plane vibrations are optically active, the band observed at 108 cm^{-1} (2 × B) is assigned to the active overtone of the vibration predicted at 50 cm^{-1} (CIS method) and at 57 cm^{-1} (TD-DFT method) for the *syn* form. Noticeably, the origin of the band recorded at 202 cm^{-1} is not clear. On one hand, it can be assigned to the combination of the 89 and 108 cm^{-1} vibrations (A + 2 × B). On the other hand, it corresponds well to the even overtone (2 × C) of the vibration computed by CIS method at 98 cm^{-1} for the *syn* rotamer (the TD-DFT computed frequency at 89 cm^{-1} does not fit perfectly to this assignment, Figure 3). The even overtone of a similar out-of-plane mode is observed for **2-PI** at 163 cm^{-1}.[6] Several observed transitions (e.g., those at 293, 321, 381, 413, 439, and 472 cm^{-1}) can be satisfactorily described by combinations of the 2 × B and/or 2 × C overtones with in-plane modes. It is interesting to note that the most active in the LIF spectrum are the vibrations related to the C2−C2′ single bond which links the indole ring with furan or thiazole moieties, i.e., the in-plane rocking, as well as out-of-plane rocking and/or torsion (Figure 3).

Similarly to **FURIN**, the intense bands of **THAIN** observed at 78 (A), 263 (D), 307 (E), 485 (F), 545 (G), 571 (H), and 596 cm^{-1} (I) are assigned to fundamentals of various in-plane vibrations (Figure 2, Table 4). The spectrum shows a progression (observed at 156 and 236 cm^{-1}) of the lowest vibrational mode corresponding to the in-plane C2−C2′ rocking vibration and its combination with the other in-plane modes (the bands at 342 and 421 cm^{-1}, as well as at 386 and 465 cm^{-1}, are assigned to the progressions of the 78 cm^{-1} vibration built on the 263 and 307 cm^{-1} fundamental transitions, respectively). The band of lower intensity recorded at 93 cm^{-1} is assigned to the even overtone of the out-of-plane C2−C2′ rocking vibrations (2 × B) computed at 50 (CIS) and 48 cm^{-1} (TD-DFT) for the *syn* form. The band at 178 cm^{-1}, similarly to **FURIN**, can be assigned either to the combination of the 78 and 93 cm^{-1} vibrations (A + 2 × B) or to the even overtone (2 × C) of the C2−C2′ torsion (which is theoretically predicted at 87 (CIS) or 72 cm^{-1} (TD-DFT) for the *syn* rotameric form). Several optically active bands represent combinations of these transitions (2 × B and A + 2 × B/or 2 × C) with various in-plane vibrations (e.g., observed at 255, 335, 355, and 396 cm^{-1}).

Vibrationally resolved DF spectra of **FURIN** and **THAIN** obtained for excitation into specific vibronic levels (SVLF) are shown in Figure 4. These spectra give information about corresponding vibrational modes in the ground and S$_1$ electronic states. Excitation into the origin of **FURIN** and into the vibronic bands corresponding to the fundamental (89
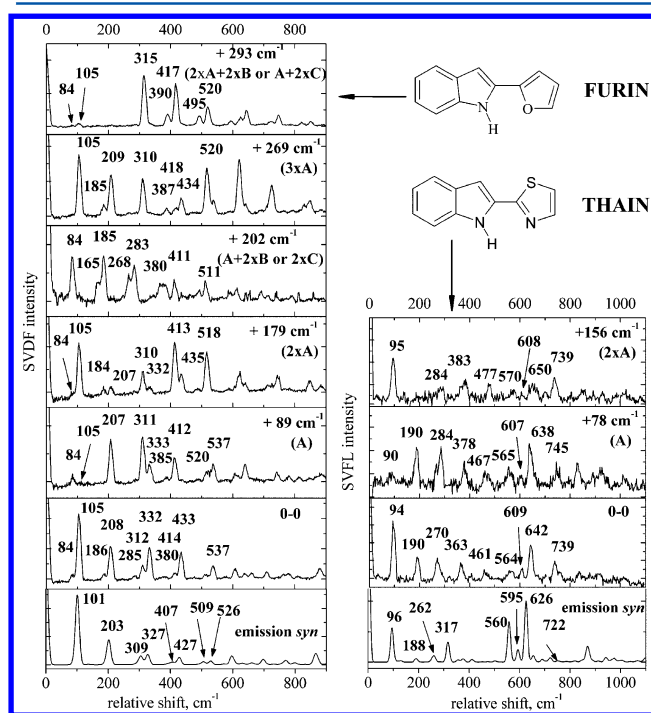
Figure 4. SVLF (top) and calculated emission (*syn* form, at the DFT/TD-DFT/B3LYP/6-31+G(d,p) level) spectra of **FURIN** (left) and **THAIN** (right). Experimental data were obtained for excitation to the origin (0−0) and to different vibronic bands corresponding to the fundamental (A) and overtone (2 × A). Additionally, SVLF **FURIN** spectra obtained for excitation to 3 × A overtone of the in-plane C2−C2′ rocking vibration as well as to the even overtone of the out-plane C2−C2′ torsional vibration (2 × C) and its combination with the in-plane A mode (293 cm^{-1}) or, depending on the interpretation, to the combinations of A and 108 cm^{-1} vibrations are presented.

Table 5. Transition Energies (cm^{-1}) and Tentative Assignments ($\Delta\tilde{\nu}_{calc}$ computed at the DFT/B3LYP/6-31+G(d,p) level) of the Vibronic Transitions ($\Delta\tilde{\nu}_{exp}$) in the Low-Energy Part of the SVLF Spectra^{b} of FURIN and THAIN

FURIN						THAIN			
excitation into the origin (0−0)		excitation into 2 × C ? (202 cm^{-1})		$\Delta\tilde{\nu}_{calc}$^{c}		excitation into the origin (0−0)		$\Delta\tilde{\nu}_{calc}$^{c}	
$\Delta\tilde{\nu}_{exp}$	assign.^{a}	$\Delta\tilde{\nu}_{exp}$	assign.	*syn*	*anti*	$\Delta\tilde{\nu}_{exp}$	assign.^{a}	*syn*	*anti*
0	0−0					0	0−0		
84	2 × C′	83	2 × C′	46 × 2	31 × 2				
105	**A′**			**101**	**103**	94	**A′**	**96**	**96**
		165	4 × C′			190	2 × **A′**		
186	**A′** + 2 × C′	185	**A′** + 2 × C′						
208	2 × **A′**	268	**A′** + 4 × C′						
~285	2 × **A′** + 2 × C′	283	2 × **A′** + 2 × C′						
312	3 × **A′** or **D′**			**309**	**306**	270	**D′**	**262**	**267**
332	**E′**			**327**	**327**	319	−		
~380	2 × **A′** + 4 × C′	~380	2 × **A′** + 4 × C′			363	**A′** + **D′**		
414	2 × C′ + **E′** or **A′** + **D′**	411	2 × C′ + **E′**			407	−		
433	**A′** + **E′**					461	2 × **A′** + **D′**		
517	2 × **A′** + **D′**					564	**G′**	**560**	**560**
537	2 × **A′** + **E′**					609	**H′**	**595**	**594**
607	**H′**			**596**	**596**	642	−		

^{a}Bold, in-plane vibrations; normal, out-of-plane vibrations. ^{b}Estimated error: 3−6 cm^{-1}.[7] ^{c}The scaling coefficient is 0.964.[25,26]

cm^{-1}) and overtones (179 and 269 cm^{-1}) of the C2−C2′ in-plane vibration (Table 5) leads to the SVLF spectra showing the prominent progression of this vibration at 105, ~208, and ~312 cm^{-1} (the last one can also originate from a long-axis in-plane stretching vibration). Thus, most probably the vibrations 89 and 105 cm^{-1} represent the same mode in the S$_1$ and S$_0$ states, respectively. On the other hand, the SVLF spectrum recorded upon excitation to the overtone of the out-of-plane vibrational band at 202 cm^{-1} shows a different pattern of the low frequency vibrations. The spectrum shows clear overtones of the 84 cm^{-1} vibrational mode (e.g., observed at 165 cm^{-1}) and combinations with the 105 cm^{-1} mode and its overtones (observed at 185, 268, 283, and ~380 cm^{-1}). It indicates that this mode at 84 cm^{-1}, which probably corresponds to the even overtone of the out-of-plane C2−C2′ torsion, increases its energy from about 42 cm^{-1} to about 101 cm^{-1} upon S$_1$ ← S$_0$ excitation. This hypothesis is supported by the analysis of charges on the furan nitrogen and indole oxygen atoms. In the ground state both of them are negatively charged. Upon electronic excitation the charge on the nitrogen atom becomes positive. This effect forces them to attract each other, which, in turn, leads to the increase of frequency of the respective out-of-plane C2−C2′ torsional mode.

The presented assignment of the corresponding vibrational modes in the ground and S$_1$ electronic states is supported by the vibrational structure of the SVLF spectrum obtained for the simultaneous excitation of the in-plane and out-of-plane modes at 293 cm^{-1} (both 84 and 105 cm^{-1} bands of similar intensity are observed in the spectrum). The computed ground and excited state vibrations of **FURIN** (Figure 3, all the data of calculations are presented in ref 27) are in agreement with the proposed correlations. The analysis of the vibrational structure of the LIF and SVLF spectra indicates that the most considerable geometry change following electronic excitation to the fluorescent state takes place along the in-plane and out-of-plane low frequency modes connected with the C2−C2′ single bond.

SVLF spectra of **THAIN** recorded for excitation into the origin and into two other vibronic levels (corresponding to the

in-plane C2−C2′ rocking vibration and its overtone) are presented in Figure 4. The bands observed at 94, 270, 564, and 609 cm^{-1} are assigned to fundamentals of the various in-plane modes (Table 5). The spectra show an overtone of the in-plane C2−C2′ rocking vibration (at 190 cm^{-1}) and several combinations (e.g., at 363 and 461 cm^{-1}). Contrary to **FURIN**, the spectra do not show any sign of the optical activity of the out-of-plane C2−C2′ vibrations, which are predicted to be observed at about 96 cm^{-1} (the first even overtone of the torsional vibration) and at about 132 cm^{-1} (the overtone of the rocking vibration). The analysis of the LIF and SVLF spectra of **THAIN** suggests that the change of its geometry takes place along the in-plane C2−C2′ rocking vibration. The frequency value of this particular mode decreases from 94 cm^{-1} to 78 cm^{-1} upon electronic excitation.

4. SUMMARY

This work presents spectroscopic and photophysical investigations and quantum chemical calculations for a series of bifunctional indole derivatives which can form *syn* and *anti* conformers via internal rotation around a single bond (**THOIN**, **THAIN**, and **FURIN**) and their comparison with the compound that does not have a hydrogen bond acceptor center (**PYRIN**). The study of solvent effects on the photophysical properties of **FURIN**, **THAIN**, and **THOIN** does not reveal any spectral or kinetic evidence of rotamerization and/or photoinduced tautomerization processes. The compounds show strongly allowed and efficient fluorescence. The lack of efficient deactivation of the lowest excited singlet states S$_1$ in protic media, either via internal conversion (IC) or ESDPT processes, can be explained by assuming that the studied compounds do not form actively quenched cyclic, doubly hydrogen-bonded complexes. The use of supersonic jet techniques combined with laser spectroscopy and TD-DFT calculation leads to the results which suggest that the *syn* rotamer is a dominant form of **THAIN** and **FURIN**. The analysis of the LIF and SVLF spectra indicates that the changes following electronic excitation are connected with the out-of-plane rocking and torsion motions along the C2−C2′

single bond that links the indole ring with the furan or thiazole moiety.

Finally, it should be stressed that the preliminary investigations of complexes of **FURIN** and **THAIN** with acetonitrile, methanol, and water under supersonic jet conditions have also been performed. The obtained LIF excitation spectra (not shown), however, are difficult to analyze without parallel investigations by resonant two-photon ionization (R2PI) and IR/R2PI ion depletion spectroscopy, combining the structurally sensitive infrared (IR) vibrational predissociation spectroscopy with the mass selective R2PI spectrometry. These laser spectroscopy/supersonic jet experiments are in progress in our laboratory.

■ AUTHOR INFORMATION

Corresponding Author
*E-mail: herbich@ichf.edu.pl. Fax: + 48 (22) 3433333.

Notes
The authors declare no competing financial interest.

■ REFERENCES

(1) Herbich, J.; Hung, C. Y.; Thummel, R. P.; Waluk, J. Solvent-Controlled Excited State Behavior: 2-(2′-Pyridyl)indoles in Alcohols. *J. Am. Chem. Soc.* **1996**, *118*, 3508−3518.

(2) Kyrychenko, A.; Herbich, J.; Wu, F.; Thummel, R. P.; Waluk, J. Solvent-Induced *Syn-Anti* Rotamerization of 2-(2′-Pyridyl)indole and the Structure of its Alcohol Complexes. *J. Am. Chem. Soc.* **2000**, *122*, 2818−2827.

(3) Waluk, J. Hydrogen-Bonding-Induced Phenomena in Bifunctional Heteroazaaromatics. *Acc. Chem. Res.* **2003**, *36*, 832−838.

(4) Kijak, M.; Zielinska, A.; Chamchoumis, C.; Herbich, J.; Thummel, R. P.; Waluk, J. Conformational Equilibria and Photoinduced Tautomerization in 2-(2′-Pyridyl)pyrrole. *Chem. Phys. Lett.* **2004**, *400*, 279−285.

(5) Kijak, M.; Petkova, I.; Toczek, M.; Wiosna-Salyga, G.; Zielinska, A.; Herbich, J.; Thummel, R. P.; Waluk, J. Conformation-Dependent Photophysics of Bifunctional Hydrogen Bond Donor/Acceptor Molecules. *Acta Phys. Pol., A* **2007**, *112*, S105−S120.

(6) Nosenko, Y.; Stepanenko, Y.; Wu, F.; Thummel, R. P.; Mordzinski, A. Laser Studies of Pyridylindoles in Supersonic Jets. *Chem. Phys. Lett.* **1999**, *315*, 87−94.

(7) Kijak, M.; Nosenko, Y.; Singh, A.; Thurnmel, R. P.; Brutschy, B.; Waluk, J. Ground and Excited State Vibrations of 2-(2 ′-Pyridyl)-pyrrole. *J. Mol. Struct.* **2007**, *844*, 286−299.

(8) Marks, D.; Zhang, H.; Borowicz, P.; Waluk, J.; Glasbeek, M. (Sub)picosecond Fluorescence Upconversion Studies of Intermolecular Proton Transfer of Dipyrido[2,3-a:3′,2′-i]carbazole and Related Compounds. *J. Phys. Chem. A* **2000**, *104*, 7167−7175.

(9) Lipinska, T. M.; Czarnocki, S. J. A New Approach to Difficult Fischer Synthesis: The Use of Zinc Chloride Catalyst in Triethylene Glycol Under Controlled Microwave Irradiation. *Org. Lett.* **2006**, *8*, 367−370.

(10) Lipinska, T. M. 1,2,4-Triazines in Organic Synthesis − Part 35 − Total Synthesis of New Indolo[2,3-a]quinolizine Alkaloids Sempervirine Type, Potential Pharmaceuticals. *Tetrahedron* **2006**, *62*, 5736−5747.

(11) Bocchi, V.; Palla, G. Synthesis and Spectroscopic Characteristics of 2,3′-Biindolyls and 2,2′-Indolylpyrroles. *Tetrahedron* **1984**, *40*, 3251−3256.

(12) Velapoldi, R. A.; Tonnesen, H. H. Corrected Emission Spectra and Quantum Yields for a Series of Fluorescent Compounds in the Visible Spectral Region. *J. Fluoresc.* **2004**, *14*, 465−472.

(13) Vdovin, A.; Sepiol, J.; Jasny, J.; Kauffman, J. M.; Mordzinski, A. Excited State Proton Transfer in Jet-Cooled 2,5-Di-(2-benzoxazolyl)-phenol. *Chem. Phys. Lett.* **1998**, *296*, 557−565.

(14) Stepanenko, Y.; Sobolewski, A. L.; Mordzinski, A. Electronic Spectroscopy and Methyl Internal Rotation Dynamics of 9,10-Dimethylanthracene. *J. Mol. Spectrosc.* **2005**, *233*, 15−22.

(15) Frisch, M. J.; Trucks, G. W.; Schlegel, H. B.; Scuseria, G. E.; Robb, M. A.; Cheeseman, J. R.; Scalmani, G.; Barone, V.; Mennucci, B.; Petersson, G. A., et al. *Gaussian 09*, Revision A.1; Gaussian, Inc.: Wallingford CT, 2010.

(16) Lee, C. T.; Yang, W. T.; Parr, R. G. Development of the Colle-Salvetti Correlation-Energy Formula into a Functional of the Electron-Density. *Phys. Rev. B* **1988**, *37*, 785−789.

(17) Becke, A. D. Density-Functional Exchange-Energy Approximation with Correct Asymptotic-Behavior. *Phys. Rev. A* **1988**, *38*, 3098−3100.

(18) McGlynn, S. P.; Azumi, T.; Kinoshita, M. *Molecular Spectroscopy of the Triplet State*; Prentice-Hall Inc.: Englewood Cliffs, NJ, 1969.

(19) Birks, J. B. *Photophysics of Aromatic Molecules*; Wiley: New York, 1978.

(20) Michl, J.; Thulstrup, E. W. *Spectroscopy with Polarized Light*; Wiley: New York, 1986.

(21) Schmidtke, S. J.; MacManus-Spencer, L. A.; Klappa, J. J.; Mobley, T. A.; McNeill, K.; Blank, D. A. 2-(2′-Pyridyl)pyrroles: Part I. Structure and Energetics of Pyridylpyrroles, Their Dimers, Complexes and Excited States. *Phys. Chem. Chem. Phys.* **2004**, *6*, 3938−3947.

(22) MacManus-Spencer, L. A.; Schmidtke, S. J.; Blank, D. A.; McNeill, K. 2-(2′-Pyridyl)pyrroles: Part II. Spectroscopic Investigation of Pyridylpyrrole Alcohol Complexes. *Phys. Chem. Chem. Phys.* **2004**, *6*, 3948−3957.

(23) Vetokhina, V.; Dobek, K.; Kijak, M.; Kaminska, I. I.; Muller, K.; Thiel, W. R.; Waluk, J.; Herbich, J. Three Modes of Proton Transfer in One Chromophore: Photoinduced Tautomerization in 2-(1H-Pyrazol-5-yl)pyridines, Their Dimers and Alcohol Complexes. *Chem. Phys. Chem.* **2012**, *13*, 3661−3671.

(24) Yu, W. S.; Cheng, C. C.; Cheng, Y. M.; Wu, P. C.; Song, Y. H.; Chi, Y.; Chou, P. T. Excited-State Intramolecular Proton Transfer in Five-Membered Hydrogen-Bonding Systems: 2-Pyridyl Pyrazoles. *J. Am. Chem. Soc.* **2003**, *125*, 10800−10801.

(25) Merrick, J. P.; Moran, D.; Radom, L. An Evaluation of Harmonic Vibrational Frequency Scale Factors. *J. Phys. Chem. A* **2007**, *111*, 11683−11700.

(26) http://cccbdb.nist.gov/vsf.asp : *Vibrational Frequency Scaling Factors*.

(27) Vetokhina, V. Ph.D. Thesis: *Spectroscopy, Photophysics, Conformational Equilibria, and Photoinduced Tautomerization in Selected Bifunctional Proton Donor-Acceptor Azaaromatic Molecules.* Institute of Physical Chemistry PAS, Warsaw, 2012. See Table S.5.1 and S.5.2 (Chapter 7, Supporting Information) - http://ichf.edu.pl/r_act/PhD-thesis/PhD-Vetokhian_suppl.pdf.

4906

dx.doi.org/10.1021/jp402767x | *J. Phys. Chem. A* 2013, 117, 4898−4906